Přírodovědecká fakulta
Faculty of Science

Jihočeská univerzita v Českých Budějovicích
University of South Bohemia in České Budějovice

# Warburg effect in lymph gland of *Drosophila melanogaster* upon parasitoid wasp infection

Laboratory of Molecular Integrative Physiology in Drosophila

DEPARTMENT OF MOLECULAR BIOLOGY

**Paul Strasser**
**Supervisor: Mgr. Tomas Dolezal, Ph.D.**

**Bachelor Thesis:** Strasser, P., 2016: Warburg effect in lymph gland of Drosophila melanogaster upon parasitoid wasp infection, Bachelor Thesis, in English – 36 pages, Department of Molecular Biology, Faculty of Science, University of South Bohemia in České Budějovice

**Annotation:** The aim of this thesis was to develop an *ex vivo* set-up for the measurement of lactate and adenosine produced by the lymph gland of *Drosophila melanogaster* and to measure the difference in concentration between infected and uninfected larvae using a parasitoid wasp infection by *Leptopilina boulardi* to further understand the metabolic switch and its needs during the onset of the immune system.

**Affirmation:** I hereby declare that I have worked on the submitted bachelor thesis independently. All additional sources are listed in the bibliography section. I hereby declare that, in accordance with Article 47b of Act No. 111/1998 in the valid wording, I agree with the publication of my bachelor thesis, in full form to be kept in the Faculty of Science archive, in electronic form in publicly accessible part of the STAG database operated by the University of South Bohemia in České Budějovice accessible through its web pages. Further, I agree to the electronic publication of the comments of my supervisor and thesis opponents and the record of the proceedings and results of the thesis defense in accordance with aforementioned Act No. 111/1998. I also agree to the comparison of the text of my thesis with the Theses.cz thesis database operated by the National Registry of University Theses and a plagiarism detection system.

Ceske Budejovice, Paul Strasser

# Table of Content

# 1 Introduction

Aerobic glycolysis, the major part of a metabolic program known as the Warburg effect, describes the use of a metabolic pathway inferior to the normally used oxidative phosphorylation concerning the pure energy production but superior regarding the metabolic rate.

The usage of a metabolic pathway applying a high rate with a low yield can be evolutionarily seen as an advantage when there is a competition for shared resources[1].

A system employing aerobic glycolysis is the immune system, which is studied in this thesis upon activation. After it is switched on it acts ”selfishly“ [2]. It relocates nutrients from the body to itself to allow an adequate response against the cause [3]. For the study of this metabolic switch, the model system of third instar larvae of *Drosophila melanogaster* was used upon immune system activation using parasitoid wasp infection. As the whole larvae run essentially on aerobic glycolysis since cells are proliferating in the growing larvae, an *in vivo* measurement is complicated, because it proves to be difficult to determine the origin of the lactate; additionally the lactate produced is transported to the fat body where it is further processed.

In order to avoid the problems related to an *in vivo* measurement of lactate, an *ex vivo* set-up was established.

# 2 Theory

## 2.1 Drosophila melanogaster

*Drosophila melanogaster*, or fruit fly, is one of the most well-known and oldest model organisms, being studied for more than a century [4]. It had and has an important role in a broad range of scientific areas like classic genetics and neuroscience, in which it served as a model for human diseases [5]. In the last few years, the *Drosophila* has been used for cancer research and studies concerned with the immune system [6,7].

Regarding studies of the immune system, a common method is the infection of *Drosophila* larvae by a parasitoid wasp. By the use of different species of parasitoid wasps, different ways of infection, and therefore, different kinds of immune response on a genetic level can be analyzed[8].

A vital organ for a general immune response of *Drosophila melanogaster* larvae upon infection is the lymph gland[9]. The lymph gland is an hematopoietic organ and origin of lamellocytes, plasmatocytes and crystal cells, which are important participants in the defense system of the host[10]. Therefore, the lymph gland and its metabolism during an immune response to a parasitoid wasp infection were investigated.

## 2.2 Leptopilina boulardi

*Leptopilina boulardi*, an endoparasitic wasp, is one of a number of different parasitoid wasp species, which uses *Drosophila melanogaster* as a host. *Leptopilina b.* is a natural parasitoid of the fruit fly and a specialized parasite of it[11,12].

The larval life cycle of *Leptopilina b.* consists of five stages, after about 26-28h a larva hatches from the stalked egg injected into the host. After around 65h, the change from first-stage larvae to second-stage larvae occurs. Alongside the pupation of the host, the larvae reach their third stage. The fourth stage occurs around 33h after the host's pupation. The larvae partially emerge from the host, transitioning from an endoparasitoid to an exoparasitoid. After 100 to 135h, the larvae's host has been consumed and they enter their fifth, prepupal stage. In a two-step process, the pupation occurs in a process spanning approximatey 18h. After a pharate adult stage the adult wasps emerge between 14 and 20 days after oviposition. The time of changes between the different stages in the life cycle depends highly on the age of the host at the injection of the egg and the sex of the emerging wasp[13].

## 2.3 Immune response of *Drosophila Melanogaster*

Alongside the eggs, the wasps inject various proteins designed to impair the fruit fly's immune response[11,14–16]. After injection, the eggs travel close to the gut and try to hide in the gut folds until they are recognized by the hemocytes, which triggers an immune response[3]. The main immune response consists of encapsulation and melanization of the parasitoid egg. First of all, the production of lamellocytes in the lymph gland is activated, resulting in a switch in metabolism. These specialized cells encapsulate the foreign egg and melanin. At the same time free radicals are released which kill the parasitoid[3,11,12,17].

Besides this main immune response, *Drosophila* also applies certain other methods to defend itself against the parasitoid. Firstly, *Drosophila melanogaster* tries to prevent the wasp from injecting its eggs by physical reactions, like rolling movements. Secondly, *Drosophila melanogaster* tries to medicate itself by producing alcohol; however, this is ineffective against *Lepopilina boulardi*. Furthermore, as soon as fruit flies recognize the presence of parasitoid wasps, they regulate their egg laying. Additionally, fruit flies undergo a symbiotic relationship with Spiroplasma parasites to gain protection against the wasp[11]. However, when the immune response fails, the wasp's larva develops. Figure 1 shows the visualization of the infection of a larva, the recognition of the egg and the the fruit fly's immune response. Figure 2 shows an egg hiding in the gut folds of a larva, recognition by lamellocytes as well as encapsulation of the parasitoid egg and a melanized egg.

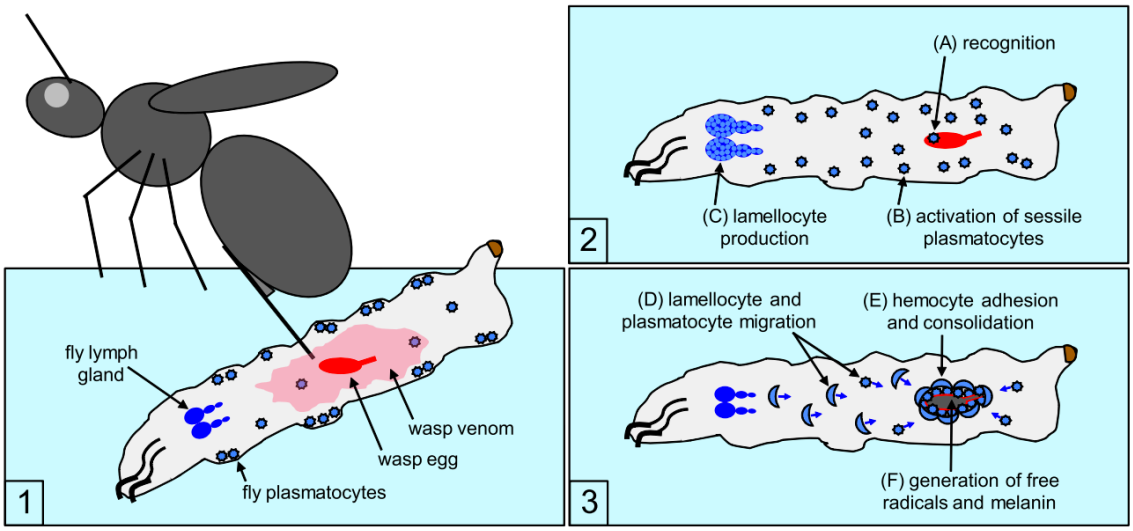


Figure 1: Graphic visualization of a parasitoid wasp infection and the immune response of the larvae; adapted from Keebaugh et al.[11]

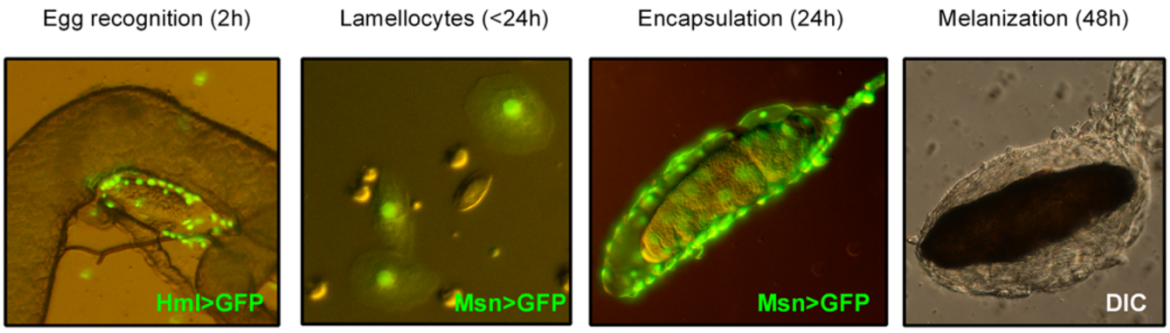


Figure 2: Immune response of the larvae against the parasitoid egg visualized via GFP tags; adapted from Bajgar et al.[3]

## 2.4 Warburg Effect

### 2.4.1 Otto Heinrich Warburg

Otto Heinrich Warburg was a German scientist, born in Freiburg in 1883. He gained a doctor's degree in chemistry in 1906 and another one in medicine in 1911. In 1931, he was awarded the Nobel Prize for his discovery of the role of iron porphyrins as respiratory enzymes, and again in 1944 for his work on fermentation but was not able to accept it due to a decree by Adolf Hitler from 1937. His further work focused on the metabolism of tumor and cancer cells and methods to cure cancer[18,19]. Therefore he formulated his own hypothesis, which is today referred to as „Warburg Hypothesis".

### 2.4.2 Warburg Hypothesis

In a lecture Warburg held at the annual meeting of Nobelists in 1966 in Lindau, Germany, he stated that:

*"All normal body cells meet their energy needs by respiration of oxygen, whereas cancer cells meet their energy needs in great part by fermentation. All normal body cells are thus obligate aerobes, whereas all cancer cells are partial anaerobes." (O. Warburg, 1966)*

Warburg investigated the metabolism of tumors and identified an exceptionally high content of fermentation of glucose to lactate for energy production. In tumor cells, energy needs are covered by fermentation by more than 50 percent; whereas, in healthy cells, no produced lactate can be detected as long as their oxygen supply is ensured and their respiration functions[20]. From this observation he concluded the Warburg Effect: Proliferating cells, like tumor cells, use the more ineffective way of energy production by means of fermentation of glucose to lactate to a greater extend without further use of the energy still present in lactate instead of oxidizing it completely like during respiration.

In further studies, he stated that all diseases have a primary cause, and therefore, also cancer must have one. Since for all cancer cells the respiration system is damaged he concluded that the change from respiration to fermentation is the prime cause for cancer and the dedifferentiation of cancer cells[21].

This extreme position had not been followed for about 35 years after Warburg's discovery; however, recently it has found interests not only in cancer research, but also in other fields like immunity[22–26].

As cancer cells are in general undifferentiated and for most unregulated proliferating cells the Warburg effect may also be used to describe the metabolism of "healthy" proliferating cells, as for example immune cells[27].

### 2.4.3 Aerobic glycolysis

The Warburg Effect describes glycolysis resulting in lactate production despite the presence of oxygen. Therefore, the term *aerobic glycolysis* was established throughout the years.

The reasons why proliferating cells utilize an, at first glance, inferior metabolic pathway to generate energy are still open to debate. Nevertheless, certain advantages are given. Although the yield of ATP from oxidation of glucose solely by aerobic glycolysis is low, the rate at which this process runs is high enough to compensate for this negative effect. In addition, the intermediates of the cycle are important precursors used for several biosynthetic pathways which are essential for proliferating cells. Again the high glycolytic rate is important, since the ability to maintain these lower-flux side pathways is highest when the main pathway runs at its maximal flux[23].

To allow this high throughput, the end-product of glycolysis, pyruvate, has to be dealt with in order to avoid an accumulation of it and therefore, a slowing down of the process. A way to fulfill this and also an explanation for aerobic glycolysis and the production of lactate was given by DeBerardinis and his colleagues[23].

The oxidation of pyruvate in the mitochondria is too slow to assure a high glycolytic flux. However, the alternative path of lactate formation is at least 200 times faster, preventing an accumulation of lactate and allowing the high-flux pathway[28,29]. Furthermore, the conversion of pyruvate to lactate by lactate dehydrogenase reoxidizes NADH, which is also necessary for the glycolytic flux[22].

To prove the usage of aerobic glycolysis by the lamellocytes of *Drosophila melanogaster* upon infection the produced lactate was measured and compared with uninfected control larvae without any immune response.

## 2.5 Adenosine as a signal for immune response

Adenosine is a metabolite of ATP, the major energy source in cells, and is produced by a cascade of different ectoenzymes. It can leave the cell as extracellular adenosine (eAdo) by equilibrative nucleoside transporters (ENTs)[3,30].

For a properly functioning immune response, a metabolic switch to aerobic glycolysis is necessary to allow the production of lamellocytes. This switch was described by Bajgar et al.[3] in three steps: First, the suppression of energy storage and developmental growth, second the retaining of more energy into circulation and lastly, the increased energy consumption by the immune system. The signal for this switch was proved to be eAdo via the use of an AdoR mutant and a parasitoid wasp infection as used for this work[3]. Extracellular adenosine acts as a hormone for glucose release[31,32] and suppresses developmental growth via adenosine receptors[3].

Adenosine was found to originate from inside the immune cells via manipulation of the ENT2 pathway by Bajgar et al.[3] indicating the privileged role of the immune system as well as the brain with exceptional high expression of the transporter supporting the idea of the selfish immune system[2].

The regulation of eAdo is faced by ADAs, adenosine deaminases, which converts it to inosine[30].In *Drosophila*, adenosine deaminase is expressed as ADGFs, adenosine deaminase-related growth factors, highly at the lymph gland as well as at the site of immune response, the melanotic capsules, encouraging the role of eAdo signaling during turned on immune system and the ineffectiveness on the immune cells itself [32,33].

To confirm the presence of eAdo further, the described methods were developed to allow a direct measurement of adenosine.

# 3 Aims

The aims of this study were to:

1. Develop a proper method for the measurement of lactate produced by the lymph gland of *Drosophila melanogaster ex vivo*.

2. Adapt the aforementioned method to enable a measurement of produced adenosine and inosine via Nanodrop spectrophotometry.

3. Measure the amount of the lactate and adenosine/inosine produced by the lymph gland of *Drosophila melanogaster* upon parasitic wasp infection by L*eptopilina boulardi* according to the established method.

# 4 Materials and Methods

## 4.1 Fly stock

The fly strain w1118 of *Drosophila melanogaster* was used for all experiments. This strain was chosen because it is commonly used in various experiments, resembling the wild type except one mutation in the white gene. Furthermore, the majority of new mutations is introduced into this strain and w1118 is used as their control suggesting a broad applicability of the method developed.

## 4.2 Parasitoid

The parasitoid wasp *Leptopilina boulardi*, described in chapter 2.2, was used for the infection of Drosophila larvae and as a trigger for the immune system.

## 4.3 Dissection media

### 4.3.1 Schneider's Drosophila Medium

Schneider's Drosophila Medium was chosen as a possible medium for dissection and *ex vivo* measurements of the lymph glands. Since it is used as a cell culture medium for *D. melanogaster* cells, it provides a broad band of different nutrients necessary for a well-functioning lymph gland.

### 4.3.2 Phosphate-buffered saline (PBS)

PBS is a commonly used buffer solution for cell cultures. It is commercially available or can be mixed in the laboratory as it was done for the experiments mentioned throughout this thesis. A pre-concentrated solution was used and diluted with distilled water.

### 4.3.3 Phosphate-buffered saline with additional sugars (PBS + sugars)

For a proper *ex vivo* measurement the dissection solution was adapted to mimic the hemolymph of the *D. melanogaster* larvae by addition of certain sugars, glucose and trehalose, to PBS. Concentrations of 200µM glucose and 6mM trehalose were chosen as measured for the hemolymph during a previous experiment performed in this laboratory. The preparation of the solutions is attached at the end of the thesis.

### 4.3.4 Phosphate-buffered saline with additional sugars and EHNA (PBS + sugars + EHNA)

To counteract adenosine deaminase present in the dissected lymph glands, and therefore, to enable a higher concentration of adenosine EHNA, erythro-9-(2-hydroxy-3-nonyl)adenine, was added to the PBS+sugars-solution.

The EHNA was purchased by Sigma Aldrich and used with different concentrations in the solution in a range from 0.015mM-0.15mM according to literature values[34–37]. The preparation of the solutions is attached at the end of the thesis.

## 4.4 Nanodrop

A Nanodrop spectrophotometer was used for the measurement of the adenosine concentration. The instrument was set for a sample type “other“ and a constant of 0. The wavelength was chosen at the maximum absorbance of adenosine at 260nm. For inosine, the wavelength was set to 235nm. At this wavelength inosine has a higher absorbance than adenosine.

## 4.5 Lactate determination

For the determination of lactate, a Lactate Assay Kit from Sigma Aldrich, catalog number MAK064, was used and the measurement was performed according to the specifications for the calorimetric detection.

## 4.6 Adenosine determination

Prior to the measurements of the adenosine release of the lymph glands the method of measurement was tested with the different dissection media and known adenosine concentrations. In addition, the different dissection media were measured against each other to evaluate differences in their absorbance at the specific wavelength. A calibration curve was constructed for the quantification of adenosine. The preparation of the solutions is attached at the end of the thesis.

## 4.7 Ex Vivo Set-up and procedure

### 4.7.1 Parasitic wasp infection

Early third instar larvae, about 72h after egg laying, were collected and infected by *Leptopilina boulardi.* The infection was tested during the dissection of the lymph gland by counting the eggs per larva. For the measurements, larvae with a number of 2-4 eggs were used.

### 4.7.2 Lymph gland dissection

The lymph glands were dissected 6h after infection. The larvae were washed several times with pure PBS and dissected in a media according to the chosen set-up. The lymph gland was then transferred to a set volume of the dissection media. The time needed for the dissections was noted down. After the number of lymph glands was collected, the solution was incubated at 25°C for a time span measured from the point the dissection of the first lymph gland started. After incubation, a specified volume of the solution was again transferred to an Eppendorf tube and stored in the freezer.

### 4.7.3 Ex Vivo Set-ups

For the preparation of the solutions used for the lactate and adenosine measurements various set-ups were tried and tested against each other to establish an optimal procedure.

Different dissection solutions, varying numbers of dissected lymph glands per sample, and different incubation times were tested as well as different volumes for the storage of the dissected lymph glands and the volume of the solution, without lymph glands, transferred into an Eppendorf tube for storage in the freezer. The methods are summarized in the tables below (Table 1, Table 2, Table 3).

Table 1: Set-ups for lactate measurements

| Method | Solution | Number of Lymph glands | V(incubation) [µL] | V (storage) [µL] | Incubation Time |
|---|---|---|---|---|---|
| Lactate-1 | Schneider's Medium | 3 | 20 | 15 | 15min |
| Lactate-2.1 | PBS+Sugars | 6 | 20 | 15 | 50min |
| Lactate-2.2 | PBS+Sugars | 6 | 20 | 15 | 2h |
| Lactate-2.3 | PBS+Sugars | 6 | 20 | 15 | 3h |

Table 2: Set-ups for adenosine measurements

| Method | Solution | EHNA Concentration [mM] | Number of Lymph glands | V(incubation) [µL] | V (storage) [µL] | Incubation Time |
|---|---|---|---|---|---|---|
| Adenosine-1.1 | PBS+Sugars | - | 3 | 20 | 4 | 30min |
| Adenosine-1.2 | PBS+Sugars | - | 3 | 20 | 4 | 1h |
| Adenosine-1.3 | PBS+Sugars | - | 3 | 20 | 4 | 1.5h |
| Adenosine-1.4 | PBS+Sugars | - | 3 | 20 | 4 | 2h |
| Adenosine-2.1 | PBS+Sugars | - | 3 | 20 | 15 | 15min |
| Adenosine-2.2 | PBS+Sugars | - | 3 | 20 | 15 | 3h |
| Adenosine-2.3 | PBS+Sugars | - | 6 | 20 | 15 | 1h |
| Adenosine-3 | PBS+Sugars+EHNA | 0.15 | 6 | 20 | 16 | 50min |
| Adenosine-4 | PBS+Sugars+EHNA | 0.15 | 1 | 10 | 8 | 1min |
| | | 0.1 | | | | 2min |
| | | 0.05 | | | | 3min |
| | | 0.025 | | | | 5min |
| | | 0.015 | | | | 8min |
| | | | | | | 10min |
| | | | | | | 15min |

Table 3: Set-ups for inosine measurements

| Method | Solution | EHNA Concentration [mM] | Number of Lymph glands | V(incubation) [µL] | V (storage) [µL] | Incubation Time |
|---|---|---|---|---|---|---|
| Inosine-1 | PBS+Sugars+EHNA | 0.15 | 1 | 10 | 8 | 1min |
| | | 0.1 | | | | 2min |
| | | 0.05 | | | | 3min |
| | | 0.025 | | | | 5min |
| | | 0.015 | | | | 8min |
| | | | | | | 10min |
| | | | | | | 15min |

# 5 Method development

To start with, an extensive training period to learn and achieve the skills essential for a successful dissection of the lymph gland and the handling of it as well as the handling of the flies and wasps was necessary. After the required dexterity was attained, several different set-ups of dissection media, dissection media volume, number of lymph glands, incubation time, and other parameters were compared with each other.

From Table 1, it can be deduced that two different dissection media were tested for the determination of lactate, Schneider's Medium was aborted after the sub-task of adenosine determination was added due to its high absorption at 260nm and the more complex composition of the medium. Instead, PBS was established as the medium of choice, enriched with glucose and trehalose in concentrations resembling the one in the larval haemolymph to allow *ex vivo* functioning of the lymph gland. The number of dissected lymph glands was increased, which can be seen by comparing the set-up of "Lactate-1" and "Lactate-2". The reason for this is based on a further increase in abilities to dissect the lymph glands in an appropriate time and to increase the lactate content in the incubated and transferred media. For the differences in incubation time between the "Lactate-2" set-ups the 2h and 3h incubation time was tested but since the 50min incubation time gave evaluable results the final method used only 50min.

The adenosine set-up was optimized according to the set-ups listed in Table 2. For Adenosine, the same increase as for lactate in numbers of lymph glands can be seen in "Adenosine-1" up to "Adenosine-3". For "Adenosine-4", the number was then decreased to one lymph gland to keep the time necessary for the dissection in accordance with the incubation times.

The incubation times for the "Adenosine-1" set-ups were each increased for 30min to see a time dependence of the adenosine content. Such a time dependence was visible; however, the long incubation times seemed impracticable. Therefore, uninfected larvae were dissected and their adenosine concentration was compared after 15min and 3h according to the set-ups "Adenosine-2.1" and "Adenosine-2.2". The increase was again visible but too high for 15min, so a middle way of an incubation time of 1h was chosen for the comparison between infected and uninfected larvae according to set-up "Adenosine-2.3". Unfortunately, the absorption for both, uninfected and infected larvae, were quite low and the instrument varied quite significantly in this range of values. To overcome this, EHNA was added to the dissection media, as stated for set-up "Adensoine-3", to inhibit adenosine deaminase, which is expressed as ADGF-A deaminase by the lymph gland as described in chapter 2.5, and increase the adenosine concentration and absorption. In an attempt to optimize the method in terms of time and since the hypothesis was stated that the adenosine concentration could be varied by the transfer in an adenosine free environment which would lead to the continuous production of adenosine by the lymph glands, the method was adapted to set-up "Adenosine-4". Just one lymph gland was used instead of six for the reason stated above and the incubation times were set between 1min and 15min to visualize the timely flow. Furthermore, the incubation volume was decreased to 10µL which was possible due to the lower number of lymph glands.

The change in transferred volume for the measurements from the incubated solution had no real influence on the measurement, since the concentration of adenosine does not depend on it and varied throughout the set-ups to either get more sample amount for measurements or speed up the process by sparing time taking less amount.

For the inosine measurements the same method as for adenosine was chosen. The Nanodrop setting, however, was adapted by altering the wave length to 235nm.

# 6 Results

The results for the lactate concentration were obtained by the Lactate Assay Kit using the colorimetric determination with a sample amount of 10µL. The calibration curve was shortened to save amount of standard solution and was adjusted to the concentrations of lactate in the sample. The absorption was measured three times, corrected according to the assay by subtracting the absorption of the blank. The average absorption was calculated; from this averaged absorption the concentration of lactate was evaluated. Two measurements were performed with a total number of 16 samples referring to a number of 96 dissected lymph glands of *Drosophila* larvae. The values for the two calibration curves, as well as the measured absorbances of the samples can be seen in Table 4-Table 7 and in Figure 7 and Figure 8 in the attachment.

For a statistical evaluation Welch's t-test was performed using the program R-Studio. This gave a p-value of 0.0488 with an average lactate concentration of 0.03899±0.001339 nmol/µL for infected larvae and $0.008051 \pm 5.157 * 10^{-5}$ nmol/µL for uninfected larvae indicating a significant difference between the lactate concentration between infected and uninfected larvae. The results are visualized in the boxplot depicted in Figure 3.

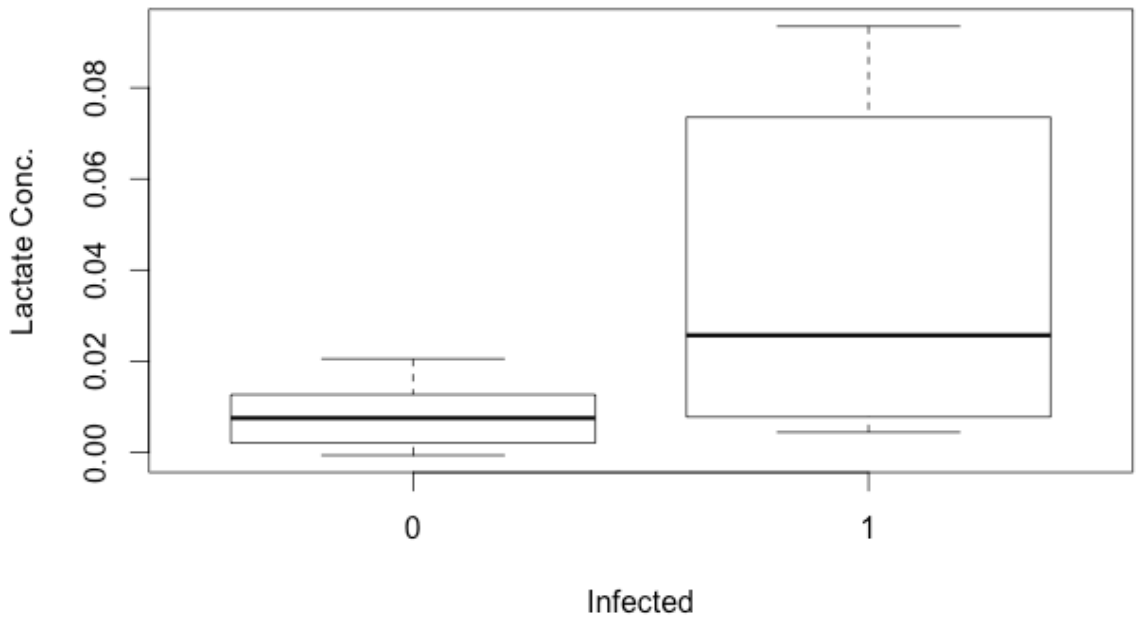


Figure 3: Boxplot visualization of the difference in lactate concentration

For the adenosine measurements different calibration curves for the varying EHNA concentrations were measured between an adenosine concentration of 0.5mM and 0.01mM. The regarding data is depicted in the attachments. Each point was measured at least three times. For the calibration curves with EHNA, concentrations of 0.05/0.025/0.015mM EHNA the calibration points for 0.35mM and 0.035mM adenosine, respectively, were excluded from the regression line. For the measurements of the adenosine concentration from the lymph gland of *Drosophila* larvae in dependence of the incubation time and EHNA concentration, the absorbance of adenosine released from seven different lymph glands were measured at least three times for each combination resulting in a total of 70 dissected lymph glands. The graphs and tables can be found in the attachment Figure 14-Figure 18 and Table 13-Table 17, and show, in general, a faster release of adenosine from lymph glands dissected from infected larvae. One exception is the graph for an EHNA concentration of 0.025mM EHNA. The reason for this could not be found.

In Figure 4 and Figure 5, it can be seen that especially with the two highest EHNA concentrations the adenosine concentration for infected larvae increases faster than for uninfected larvae and also reaches higher values (above 0.100mM), demonstrating the higher release of adenosine from infected lymph glands. In addition, they show that one needs to effectively inhibit the activity of the deaminase to be able to see clear differences since for lower EHNA concentrations these are not as clear as for the highest two, most likely due to the deaminase still converting eAdo. Furthermore, these observations can be only seen in the short time period of 10min after the dissection.

For inosine, only the absorbance was measured and no calibration curve was constructed to calculate the concentrations. No continuous interpretation of the results for the different EHNA concentrations and between infected and uninfected larvae was possible, the measurements are not depicted in this thesis.

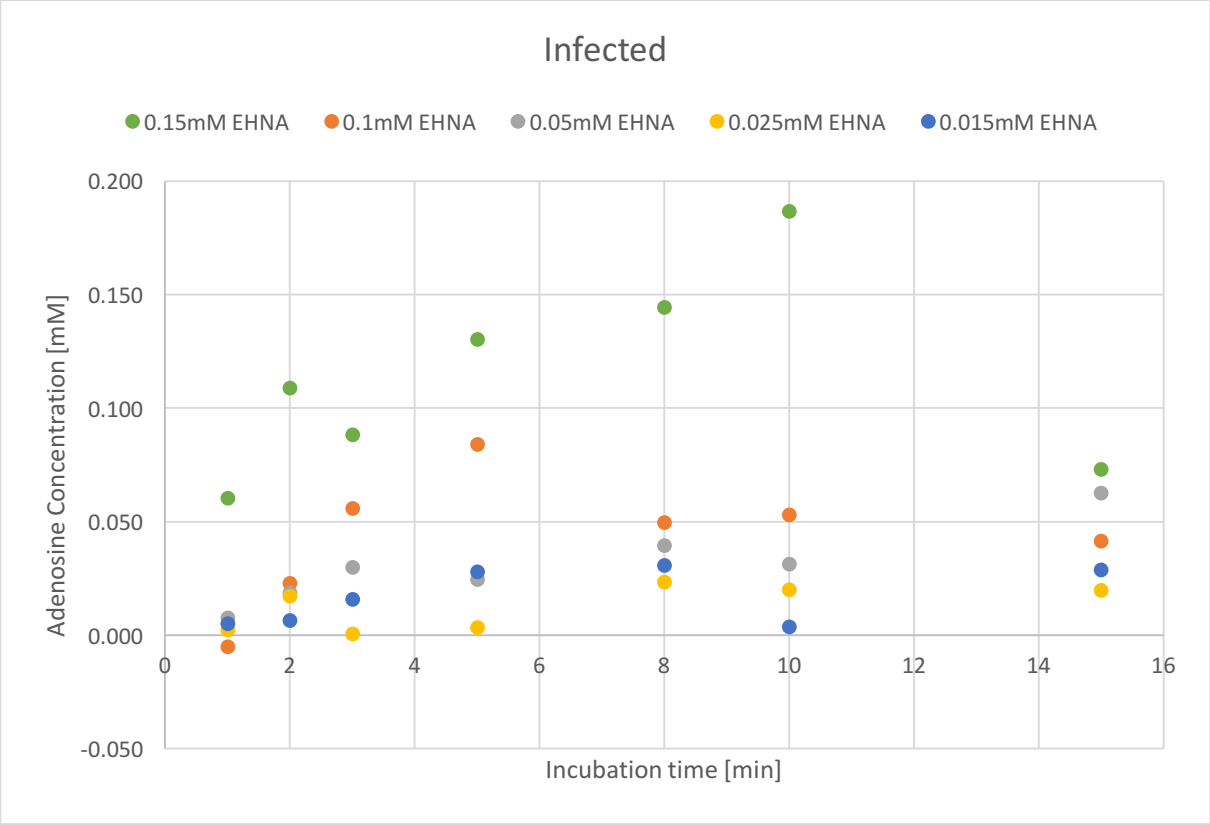


Figure 4: Comparison of adenosine concentrations after certain incubation times for different EHNA concentrations and lymph glands from infected larvae

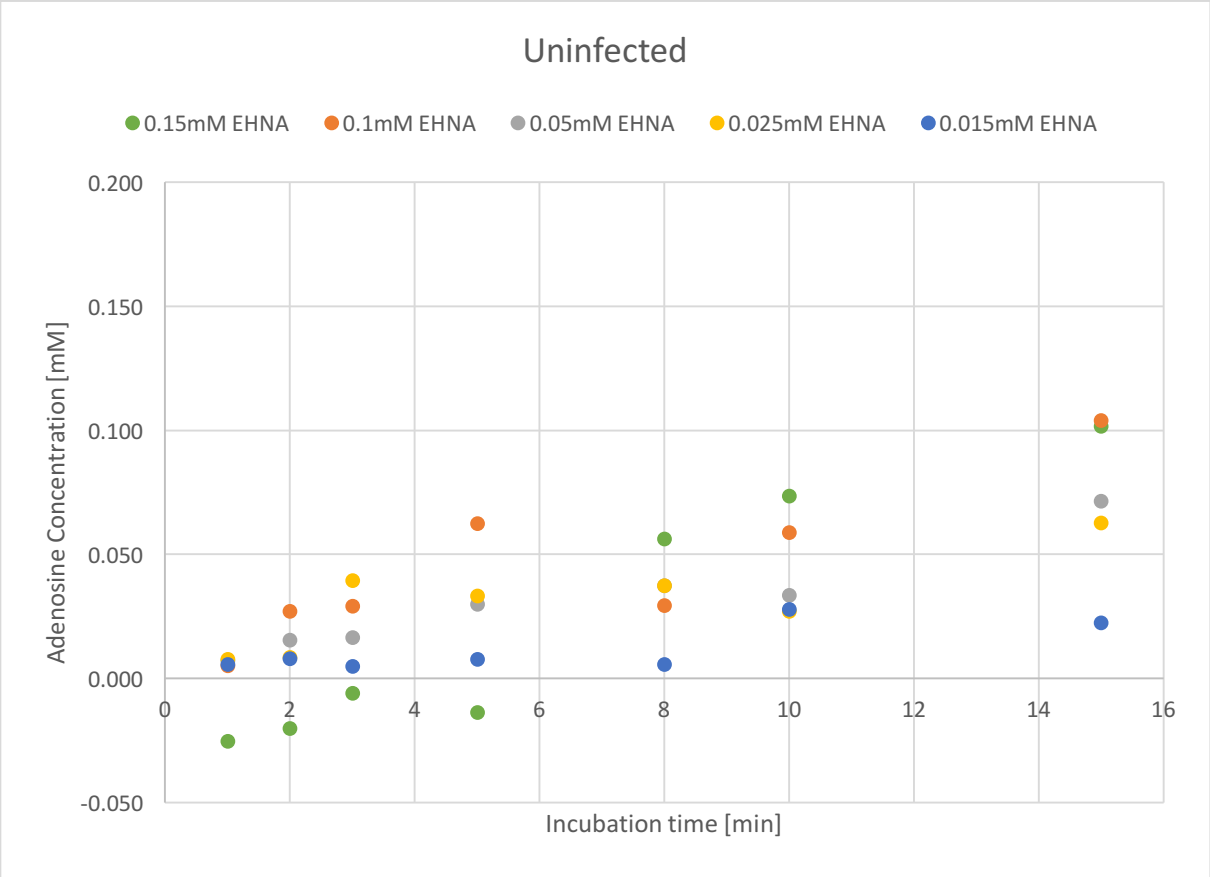


Figure 5: Comparison of adenosine concentrations after certain incubation times for different EHNA concentrations and lymph glands from uninfected larvae

# 7 Discussion

During this work, an *ex vivo* set-up for the measurements of the metabolites lactate and adenosine from lymph glands dissected from *Drosophila melanogaster* larvae was described for the first time. Furthermore, the method was applied to measure the differences of lactate and adenosine concentrations between infected and uninfected larvae using a parasitoid wasp infection with *Leptopilina boulardi*.

Although we were able to suppress the metabolic switch in a previous experiment by knocking down the Ado transporter in the lymph gland, it was now possible to prove directly the role of adenosine by measuring the actual Ado release from the lymph gland. The results show a significant difference between infected and uninfected larvae in regard of lactate and adenosine concentration with a higher concentration of both for infected larvae supporting the hypothesis of a metabolic switch to aerobic glycolysis upon infection and onset of the immune system and adenosine as the signal origin for this metabolic switch[3,22,24,27].

For further investigation, the usability of another method to measure the metabolite concentrations besides spectral analysis could be tested, namely the usage of GC-MS allowing a lower LOD and faster measurements of the high sample amount in addition with the possibility to measure more metabolites simultaneously[38,39].

All in all, the targets for research in the field of the metabolism of active immune cells and the pathways can be summed up in Figure 6, obtained from Mgr. Tomas Dolezal, Ph.D.

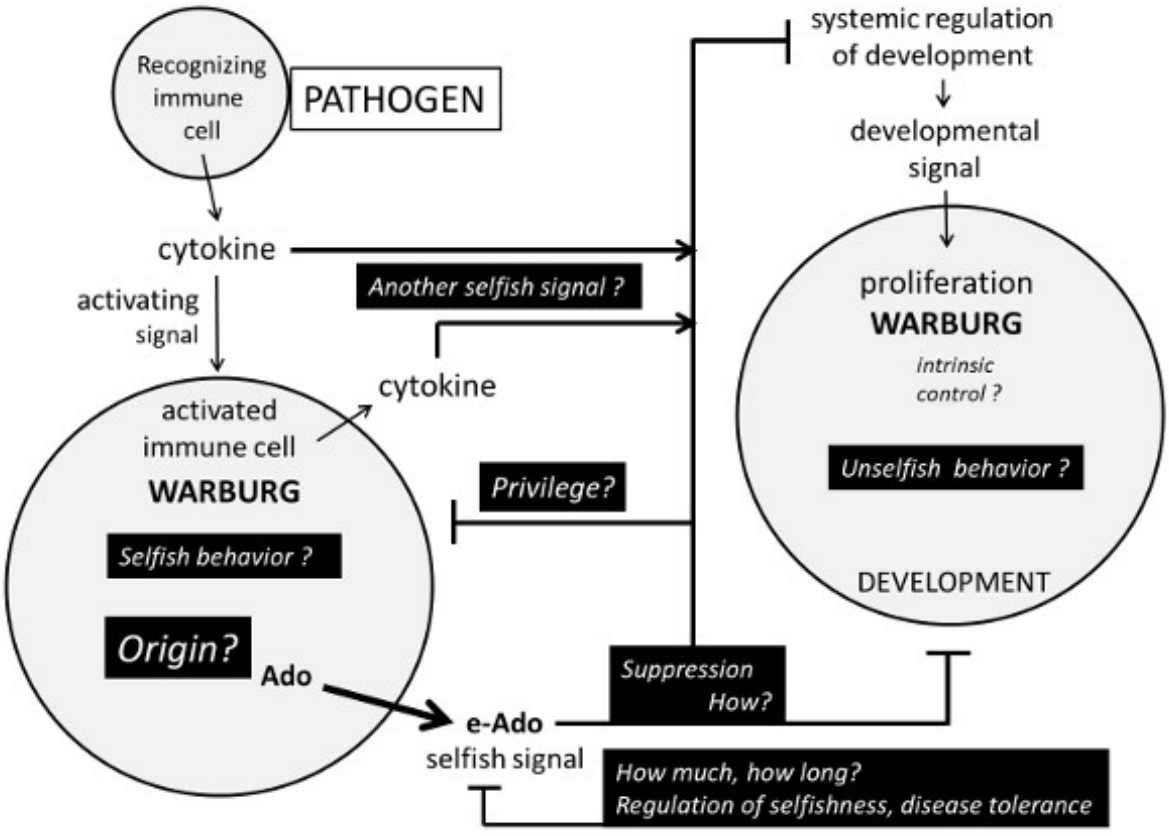


Figure 6: Pathway of the metabolic switch during immune response and further targets of investigation

# 8 References


1. Pfeiffer, T., Schuster, S. & Bonhoeffer, S. Cooperation and competition in the evolution of ATP-producing pathways. *Science* **292,** 504–507 (2001).
2. Straub, R. H. Insulin resistance, selfish brain, and selfish immune system: an evolutionarily positively selected program used in chronic inflammatory diseases. *Arthritis Res. Ther.* **16 Suppl 2,** S4 (2014).
3. Bajgar, A. *et al.* Extracellular adenosine mediates a systemic metabolic switch during immune response. *PLoS Biol.* **13,** e1002135 (2015).
4. Stephenson, R. & Metcalfe, N. H. Drosophila melanogaster: a fly through its history and current use. *J. R. Coll. Physicians Edinb.* **43,** 70–5 (2013).
5. Marsh, J. L. & Thompson, L. M. Drosophila in the Study of Neurodegenerative Disease. *Neuron* **52,** 169–178 (2006).
6. Pandey, U. B. & Nichols, C. D. Human Disease Models in Drosophila melanogaster and the Role of the Fly in Therapeutic Drug Discovery. *Drug Deliv.* **63,** 411–436 (2011).
7. Evans, C. J., Hartenstein, V. & Banerjee, U. Thicker Than Blood: Conserved Mechanisms in Drosophila and Vertebrate Hematopoiesis. *Dev. Cell* **5,** 673–690 (2003).
8. Schlenke, T. A., Morales, J., Govind, S. & Clark, A. G. Contrasting infection strategies in generalist and specialist wasp parasitoids of Drosophila melanogaster. *PLoS Pathog.* **3,** 1486–1501 (2007).
9. Sorrentino, R. P., Carton, Y. & Govind, S. Cellular Immune Response to Parasite Infection in the Drosophila Lymph Gland Is Developmentally Regulated. **80,** 65–80 (2002).
10. Lemaitre, B. & Hoffmann, J. The host defense of Drosophila melanogaster. *Annu. Rev. Immunol.* **25,** 697–743 (2007).
11. Keebaugh, E. S. & Schlenke, T. A. Insights from natural host–parasite interactions: The Drosophila model. *Dev. Comp. Immunol.* **42,** 111–123 (2014).
12. Carton, Y., Bouletreau, M., Van Alphen, J. J. M. & Van Lenteren, J. C. The Drosophila Parasitic Wasps.
13. Kopelman, A. H. & Chabora, P. C. Immature stages of Leptopilina boulardi (Hymenoptera: Eucoilidae), a protelean parasite of Drosophila spp. (Diptera: Drosophilidae). *Ann. Entomol. Soc. Am.* **77,** 264–269 (1984).
14. Colinet, D., Schmitz, A., Depoix, D., Crochard, D. & Poirié, M. Convergent Use of RhoGAP Toxins by Eukaryotic Parasites and Bacterial Pathogens. *PLoS Pathog.* **3,** e203 (2007).
15. Colinet, D. *et al.* A serpin from the parasitoid wasp Leptopilina boulardi targets the Drosophila phenoloxidase cascade. *Dev. Comp. Immunol.* **33,** 681–689 (2009).
16. Colinet, D., Cazes, D., Belghazi, M., Gatti, J.-L. & Poirie, M. Extracellular Superoxide Dismutase in Insects: CHARACTERIZATION, FUNCTION, AND INTERSPECIFIC VARIATION IN PARASITOID WASP VENOM. *J. Biol. Chem.* **286,** 40110–40121 (2011).
17. Carton, Y., Poiri??, M. & Nappi, A. J. Insect immune resistance to parasitoids. *Insect Sci.* **15,** 67–87 (2008).
18. Brand, R. A. Biographical sketch: Otto Heinrich Warburg, PhD, MD. *Clin. Orthop. Relat. Res.* **468,** 2831–2832 (2010).
19. Kyle, R. A. & Shampo, M. A. Otto Heinrich Warburg. *Mayo Clin. Proc.* **63,** 79 (1988).
20. Warburg, O., Wind, F. & Negelein, E. The Metabolism of Tumors in the Body. *J Gen Physiol*. **8**(6), 619-530 (1926).
21. Warburg, O. On the Origin of Cancer Cells. *Crit. Rev. Oncog.* **123,** 309–314 (1956).

22. Bauer, D. E. *et al.* Cytokine stimulation of aerobic glycolysis in hematopoietic cells exceeds proliferative demand. **18,** 1303–1305 (2015).
23. DeBerardinis, R. J., Lum, J. J., Hatzivassiliou, G. & Thompson, C. B. The Biology of Cancer: Metabolic Reprogramming Fuels Cell Growth and Proliferation. *Cell Metab.* **7,** 11–20 (2008).
24. Cheng, S.-C. *et al.* mTOR/HIF1α-mediated aerobic glycolysis as metabolic basis for trained immunity. **345,** 1–18 (2014).
25. Gatenby, R. A. & Gillies, R. J. Why do cancers have high aerobic glycolysis? *Nat. Rev. Cancer* **4,** 891–899 (2004).
26. Garber, K. Energy Boost : The Warburg Effect. *J. Natl. Cancer Inst.* **96,** 1805–1806 (2004).
27. Vander Heiden, M., Cantley, L. & Thompson, C. Understanding the Warburg effect: The metabolic Requiremetns of cell proliferation. *Science (80-. ).* **324,** 1029–1033 (2009).
28. Newsholme, P., Curi, R., Gordon, S. & Newsholme, E. A. Metabolism of glucose, glutamine, long-chain fatty acids and ketone bodies by murine macrophages. *Biochem. J.* **239,** 121–5 (1986).
29. Curi, R., Newsholme, P. & Newsholme, E. A. Metabolism of pyruvate by isolated rat mesenteric lymphocytes, lymphocyte mitochondria and isolated mouse macrophages. *Biochem. J.* **250,** 383–388 (1988).
30. Bours, M. J. L., Swennen, E. L. R., Di Virgilio, F., Cronstein, B. N. & Dagnelie, P. C. Adenosine 5′-triphosphate and adenosine as endogenous signaling molecules in immunity and inflammation. *Pharmacol. Ther.* **112,** 358–404 (2006).
31. Cortés, D., Guinzberg, R., Villalobos-Molina, R. & Piña, E. Evidence that endogenous inosine and adenosine-mediated hyperglycaemia during ischaemia-reperfusion through A $_3$ adenosine receptors. *Auton. Autacoid Pharmacol.* **29,** 157–164 (2009).
32. Novakova, M. & Dolezal, T. Expression of Drosophila Adenosine Deaminase in Immune Cells during Inflammatory Response. *PLoS One* **6,** e17741 (2011).
33. Zurovec, M., Dolezal, T., Gazi, M., Pavlova, E. & Bryant, P. J. Adenosine deaminase-related growth factors stimulate cell proliferation in Drosophila by depleting extracellular adenosine. *Proc. Natl. Acad. Sci. U. S. A.* **99,** 4403–8 (2002).
34. *Functional Nucleic Acids for Analytical Applications*. (Springer-Verlag New York, 2009). doi:10.1007/978-0-387-73711-9
35. Duncan, G. S., Wolberg, G., Schmitges, C. J., Deeprose, R. D. & Zimmerman, T. P. Inhibition of lymphocyte-mediated cytolysis and cyclic AMP phosphodiesterase by erythro-9-(2-hydroxy-3-nonyl)adenine. *J. Immunopharmacol.* **4,** 79–100 (1982).
36. Carson, D. A. & Seegmiller, J. E. Effect of adenosine deaminase inhibition upon human lymphocyte blastogenesis. *J. Clin. Invest.* **57,** 274–82 (1976).
37. Zavialov, A. V. *et al.* Human adenosine deaminase 2 induces differentiation of monocytes into macrophages and stimulates proliferation of T helper cells and macrophages. *J. Leukoc. Biol.* **88,** 279–290 (2010).
38. Villas-Bôas, S. G., Smart, K. F., Sivakumaran, S. & Lane, G. a. Alkylation or Silylation for Analysis of Amino and Non-Amino Organic Acids by GC-MS? *Metabolites* **1,** 3–20 (2011).
39. Smart, K. F., Aggio, R. B. M., Van Houtte, J. R. & Villas-Bôas, S. G. Analytical platform for metabolome analysis of microbial cells using methyl chloroformate derivatization followed by gas chromatography-mass spectrometry. *Nat. Protoc.* **5,** 1709–1729 (2010).
40. Rao, A. & Hogan, P. G. Calcium signaling in cells of the immune and hematopoietic systems. *Immunol. Rev.* **231,** 5–9 (2009).

# 9 Attachments

Table 4: Measured values for the calibration curve of the first lactate measurement

| Lactate Content [nmol/well] | Absorption (A570nm); Measurement: | | | Absorption (A570nm) corrected; Measurement: | | | Absorption (A570nm) averaged |
|---|---|---|---|---|---|---|---|
| | 1 | 2 | 3 | 1 | 2 | 3 | |
| 0 | 0.0668 | 0.0772 | 0.0772 | 0.0000 | 0.0000 | 0.0000 | 0.0000 |
| 2 | 0.3043 | 0.3162 | 0.3184 | 0.2375 | 0.2390 | 0.2412 | 0.2392 |
| 6 | 0.7134 | 0.7282 | 0.7282 | 0.6466 | 0.6510 | 0.6510 | 0.6495 |
| 10 | 1.1372 | 1.1655 | 1.1623 | 1.0704 | 1.0883 | 1.0851 | 1.0813 |

Table 5: Measured values for the first lactate measurement; 0=uninfected, 1=infected

| Infection | Absorption (A570nm); Measurement: | | | Absorption (A570nm) corrected; Measurement: | | | Absorption (A570nm) averaged | Lactate Concentration [nmol/µL] |
|---|---|---|---|---|---|---|---|---|
| | 1 | 2 | 3 | 1 | 2 | 3 | | |
| 0 | 0.1008 | 0.1080 | 0.1091 | 0.0340 | 0.0308 | 0.0319 | 0.0322 | 0.0205 |
| 0 | 0.0915 | 0.1032 | 0.1041 | 0.0247 | 0.0260 | 0.0269 | 0.0259 | 0.0146 |
| 0 | 0.0810 | 0.0884 | 0.1006 | 0.0142 | 0.0112 | 0.0234 | 0.0163 | 0.0056 |
| 1 | 0.1678 | 0.1924 | 0.1922 | 0.1010 | 0.1152 | 0.1150 | 0.1104 | 0.0935 |
| 1 | 0.1032 | 0.1193 | 0.1203 | 0.0364 | 0.0421 | 0.0431 | 0.0405 | 0.0283 |
| 1 | 0.1306 | 0.1525 | 0.1549 | 0.0638 | 0.0753 | 0.0777 | 0.0723 | 0.0579 |

Table 6: Measured values for the calibration curve of the second lactate measurement

| Lactate Content [nmol/well] | Absorption (A570nm); Measurement: | | | Absorption (A570nm) corrected; Measurement: | | | Absorption (A570nm) averaged |
|---|---|---|---|---|---|---|---|
| | 1 | 2 | 3 | 1 | 2 | 3 | |
| 0 | 0.0519 | 0.0517 | 0.0541 | 0.0000 | 0.0000 | 0.0000 | 0.0000 |
| 1 | 0.2171 | 0.2130 | 0.2123 | 0.1652 | 0.1613 | 0.1582 | 0.1616 |
| 2 | 0.3371 | 0.3345 | 0.3273 | 0.2852 | 0.2828 | 0.2732 | 0.2804 |
| 3 | 0.4358 | 0.4324 | 0.4276 | 0.3839 | 0.3807 | 0.3735 | 0.3794 |

Table 7: Measured values for the second lactate measurement; 0=uninfected, 1=infected

| Infection | Absorption (A570nm); Measurement: | | | Absorption (A570nm) corrected; Measurement: | | | Absorption (A570nm) averaged | Lactate Concentration [nmol/µL] |
|---|---|---|---|---|---|---|---|---|
| | 1 | 2 | 3 | 1 | 2 | 3 | | |
| 0 | 0.0818 | 0.0851 | 0.0817 | 0.0299 | 0.0334 | 0.0276 | 0.0303 | 0.0107 |
| 0 | 0.0787 | 0.0696 | 0.0693 | 0.0268 | 0.0179 | 0.0152 | 0.0200 | 0.0025 |
| 0 | 0.0664 | 0.0672 | 0.0721 | 0.0145 | 0.0155 | 0.0180 | 0.0160 | -0.0006 |
| 1 | 0.0992 | 0.1024 | 0.0936 | 0.0473 | 0.0507 | 0.0395 | 0.0458 | 0.0231 |
| 1 | 0.1672 | 0.1696 | 0.2076 | 0.1153 | 0.1179 | 0.1535 | 0.1289 | 0.0892 |
| 1 | 0.0776 | 0.0744 | 0.0727 | 0.0257 | 0.0227 | 0.0186 | 0.0223 | 0.0044 |
| 1 | 0.0862 | 0.0809 | 0.0813 | 0.0343 | 0.0292 | 0.0272 | 0.0302 | 0.0107 |
| 0 | 0.0802 | 0.0821 | 0.0813 | 0.0283 | 0.0304 | 0.0272 | 0.0286 | 0.0094 |
| 1 | 0.0919 | 0.0674 | 0.0672 | 0.0400 | 0.0157 | 0.0131 | 0.0229 | 0.0049 |
| 0 | 0.0784 | 0.0678 | 0.0679 | 0.0265 | 0.0161 | 0.0138 | 0.0188 | 0.0016 |

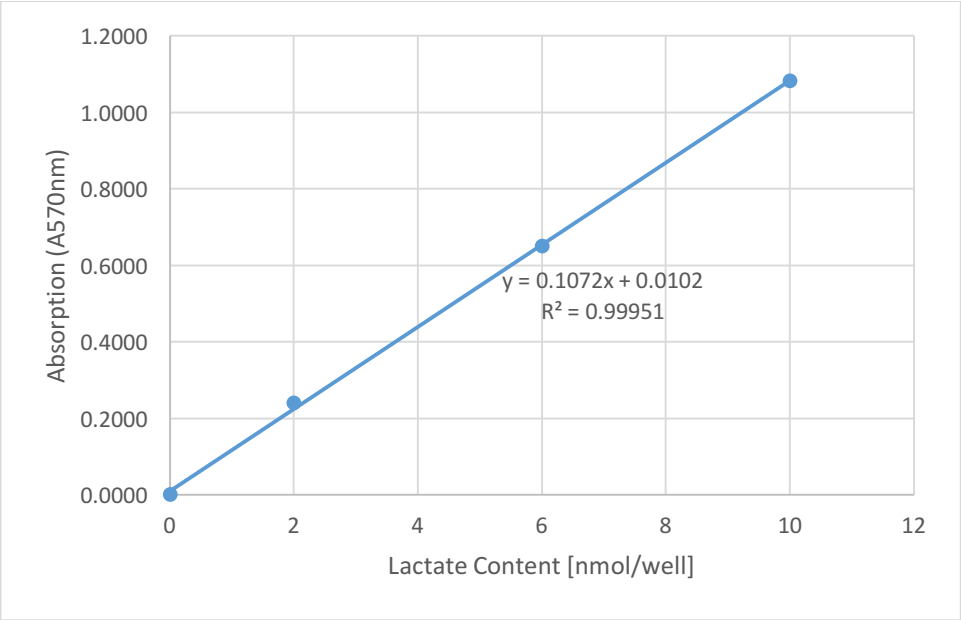


Figure 7: Calibration curve for the first lactate measurement

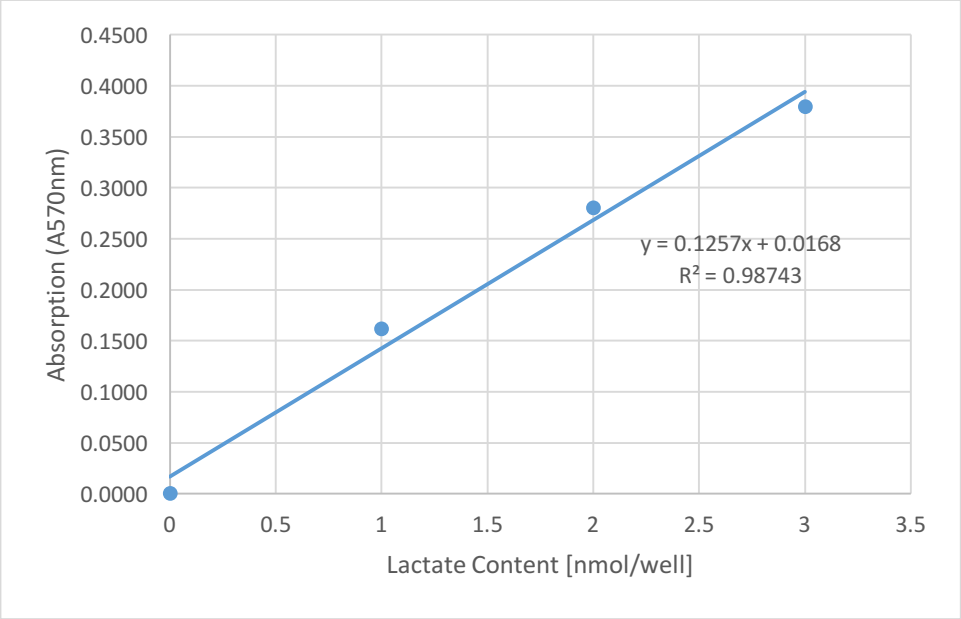


Figure 8: Calibration curve of the second lactate measurement

Table 8: Measured values for the adenosine calibration curve for 0.15mM EHNA

| Adenosine Concentration [mM] | Absorption (A260nm); Measurement: | | | Absorption (A260nm) averaged |
|---|---|---|---|---|
| | 1 | 2 | 3 | |
| 0.5 | 5.384 | 5.331 | 5.328 | 5.348 |
| 0.35 | 4.092 | 4.147 | 4.141 | 4.127 |
| 0.25 | 3.002 | 3.012 | 3.098 | 3.037 |
| 0.1 | 1.160 | 1.076 | 1.185 | 1.140 |
| 0.08 | 0.602 | 0.766 | 0.709 | 0.692 |
| 0.05 | 0.678 | 0.682 | 0.776 | 0.712 |
| 0.01 | 0.210 | 0.248 | 0.331 | 0.263 |

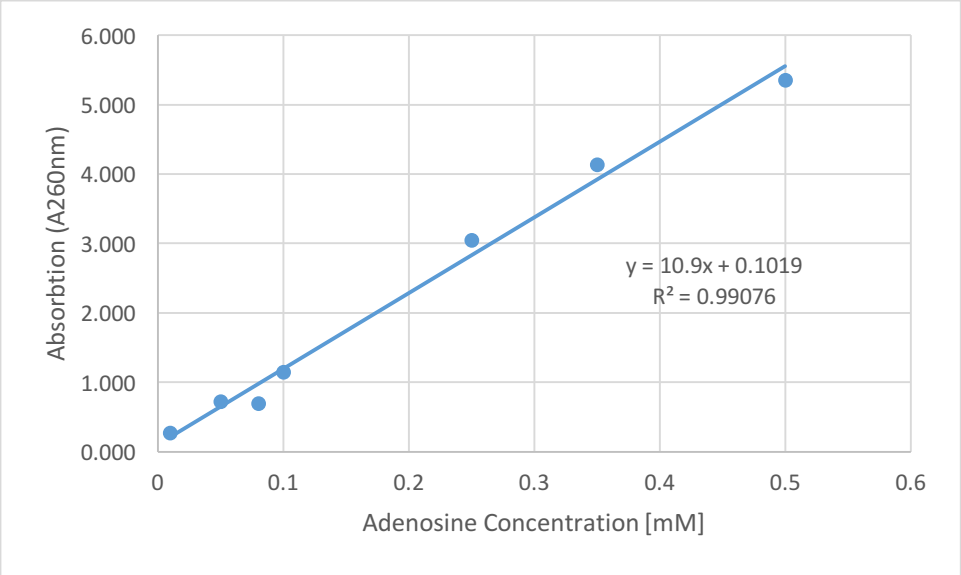


Figure 9: Adenosine calibration curve for 0.15mM EHNA

Table 9: Measured values for the adenosine calibration curve for 0.1mM EHNA

| Adenosine Concentration [mM] | Absorption (A260nm); Measurement: | | | | | Absorption (A260nm) averaged |
|---|---|---|---|---|---|---|
| | 1 | 2 | 3 | 4 | 5 | |
| 0.5 | 5.297 | 5.213 | 5.343 | - | - | 5.284 |
| 0.35 | 3.803 | 3.846 | 3.939 | - | - | 3.863 |
| 0.25 | 2.723 | 2.673 | 2.797 | - | - | 2.731 |
| 0.1 | 1.124 | 1.147 | 1.229 | - | - | 1.167 |
| 0.08 | 0.894 | 0.927 | 0.933 | - | - | 0.918 |
| 0.05 | 0.475 | 0.561 | 0.580 | - | - | 0.539 |
| 0.01 | 0.369 | 0.504 | 0.175 | 0.302 | 0.557 | 0.381 |

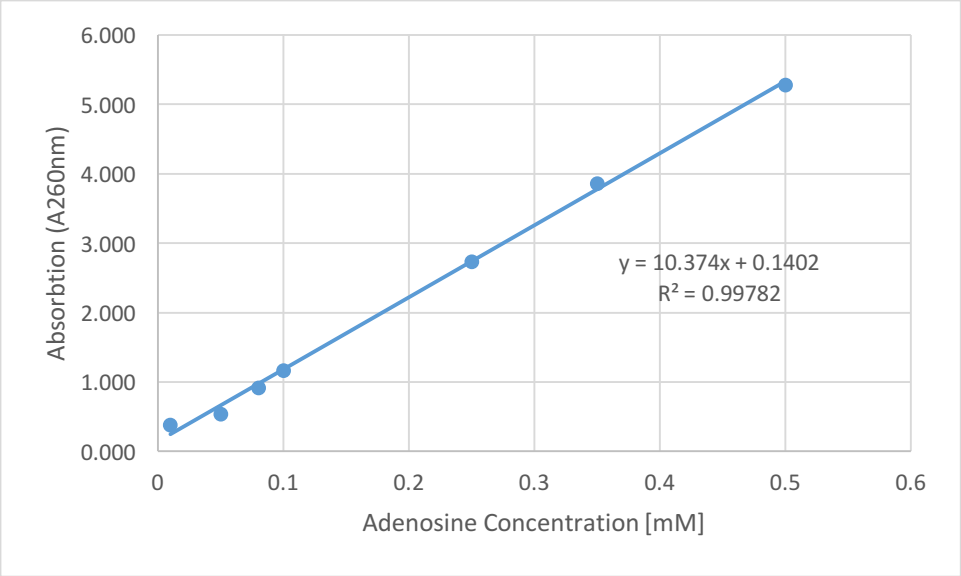


Figure 10: Adenosine calibration curve for 0.1mM EHNA

Table 10: Measured values for the adenosine calibration curve for 0.05mM EHNA

| Adenosine Concentration [mM] | Absorption (A260nm); Measurement: | | | Absorption (A260nm) averaged |
|---|---|---|---|---|
| | 1 | 2 | 3 | |
| 0.5 | 5.231 | 5.281 | 5.331 | 5.281 |
| 0.35 | 1.622 | 1.685 | 1.653 | 1.653 |
| 0.25 | 2.934 | 2.896 | 2.986 | 2.939 |
| 0.1 | 1.087 | 1.089 | 1.091 | 1.089 |
| 0.08 | 0.770 | 0.733 | 0.798 | 0.767 |
| 0.05 | 0.388 | 0.047 | 0.432 | 0.289 |
| 0.01 | 0.058 | 0.118 | 0.055 | 0.077 |

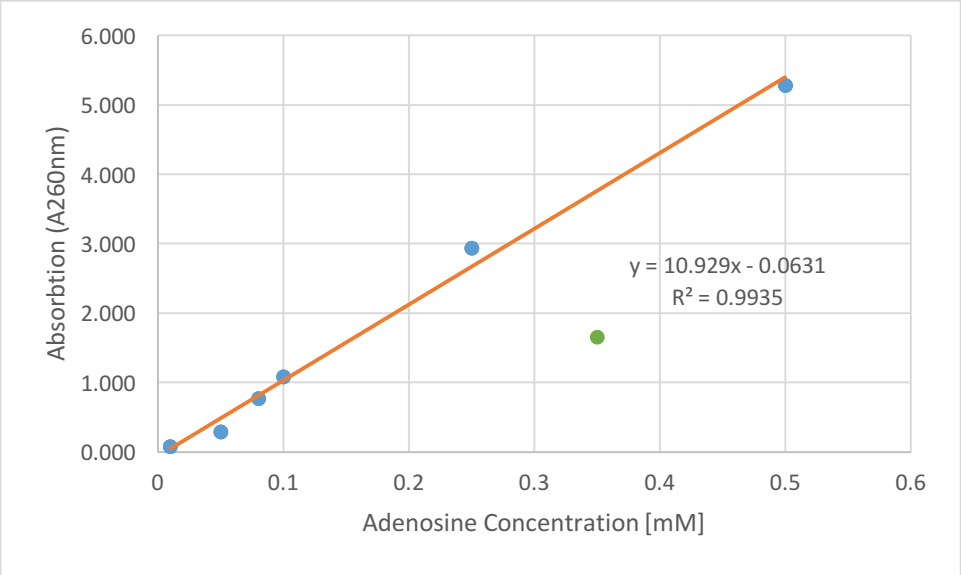


Figure 11: Adenosine calibration curve for 0.05mM EHNA; the value for 0.34mM adenosine was excluded from the regression

Table 11: Measured values for the adenosine calibration curve for 0.025mM EHNA

| Adenosine Concentration [mM] | Absorption (A260nm); Measurement: | | | Absorption (A260nm) averaged |
|---|---|---|---|---|
| | 1 | 2 | 3 | |
| 0.5 | 5.438 | 5.345 | 5.480 | 5.421 |
| 0.35 | 1.475 | 1.467 | 1.463 | 1.468 |
| 0.25 | 2.797 | 2.790 | 2.915 | 2.834 |
| 0.1 | 1.116 | 1.186 | 1.128 | 1.143 |
| 0.08 | 0.889 | 0.893 | 0.908 | 0.897 |
| 0.05 | 0.535 | 0.504 | 0.481 | 0.507 |
| 0.01 | 0.151 | 0.124 | 0.172 | 0.149 |

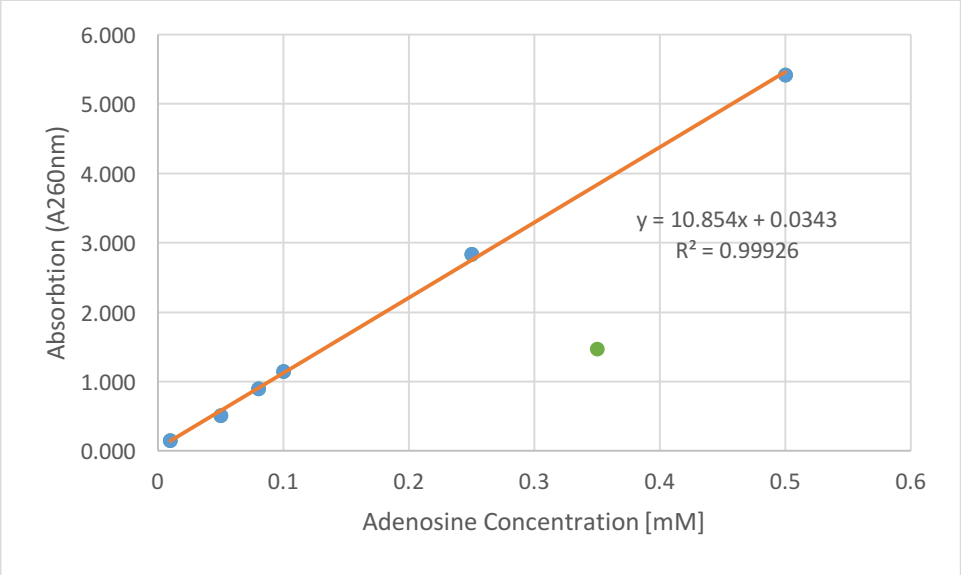


Figure 12: Adenosine calibration curve for 0.025mM EHNA; the value for 0.35mM adenosine was excluded from regression

Table 12: Measured values for the adenosine calibration curve for 0.015mM EHNA

| Adenosine Concentration [mM] | Absorption (A260nm); Measurement: | | | | Absorption (A260nm) averaged |
|---|---|---|---|---|---|
| | 1 | 2 | 3 | 4 | |
| 0.05 | 0.556 | 0.607 | 0.668 | - | 0.610 |
| 0.035 | 0.112 | 0.112 | 0.124 | - | 0.116 |
| 0.025 | 0.242 | 0.316 | 0.301 | 0.291 | 0.288 |
| 0.01 | 0.103 | 0.091 | 0.106 | - | 0.100 |

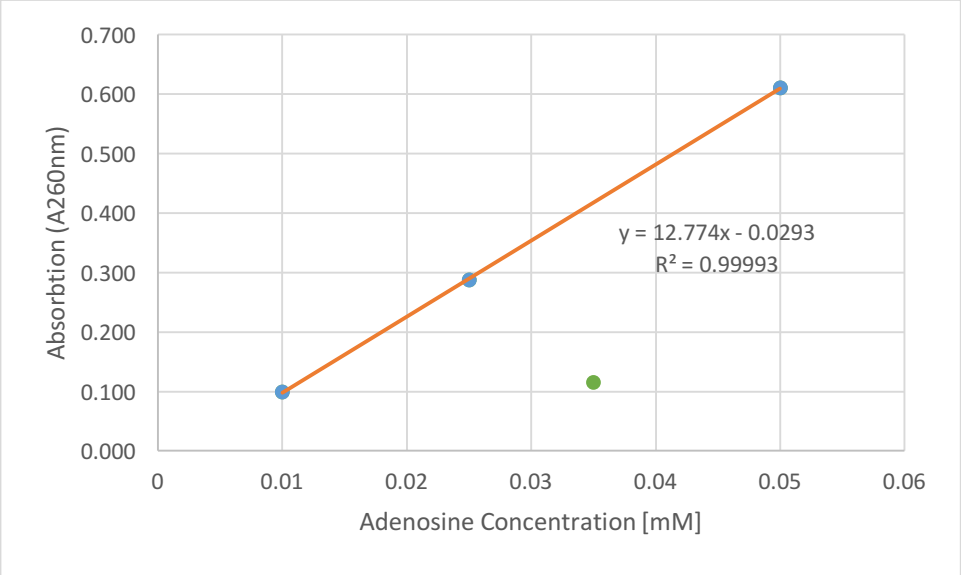


Figure 13: Adenosine calibration curve for 0.015mM EHNA; the value for 0.035mM adenosine was excluded from regression

Table 13: Measured values of the adenosine concentrations in dependence of time for 0.15mM EHNA

| Infection | Incubation time [min] | Absorption (A570nm); Measurement: | | | | | Absorption (A570nm) averaged | Adenosine Concentration [mM] |
|---|---|---|---|---|---|---|---|---|
| | | 1 | 2 | 3 | 4 | 5 | | |
| 0 | 1 | -0.206 | -0.090 | -0.102 | -0.252 | -0.209 | -0.172 | -0.025 |
| 0 | 2 | -0.124 | -0.109 | -0.116 | - | - | -0.116 | -0.020 |
| 0 | 3 | -0.058 | 0.072 | 0.102 | - | - | 0.039 | -0.006 |
| 0 | 5 | -0.139 | -0.116 | 0.120 | - | - | -0.045 | -0.013 |
| 0 | 8 | 0.611 | 0.726 | 0.810 | - | - | 0.716 | 0.056 |
| 0 | 10 | 0.771 | 0.977 | 0.965 | - | - | 0.904 | 0.074 |
| 0 | 15 | 0.510 | 1.496 | 1.623 | - | - | 1.210 | 0.102 |
| 1 | 1 | 0.635 | 0.813 | 0.833 | - | - | 0.760 | 0.060 |
| 1 | 2 | 1.073 | 1.166 | 1.625 | - | - | 1.288 | 0.109 |
| 1 | 3 | 0.838 | 1.153 | 1.199 | - | - | 1.063 | 0.088 |
| 1 | 5 | 1.394 | 1.553 | 1.617 | - | - | 1.521 | 0.130 |
| 1 | 8 | 1.559 | 1.685 | 1.787 | - | - | 1.677 | 0.145 |
| 1 | 10 | 1.929 | 2.084 | 2.396 | - | - | 2.136 | 0.187 |
| 1 | 15 | 0.826 | 0.900 | 0.964 | - | - | 0.897 | 0.073 |

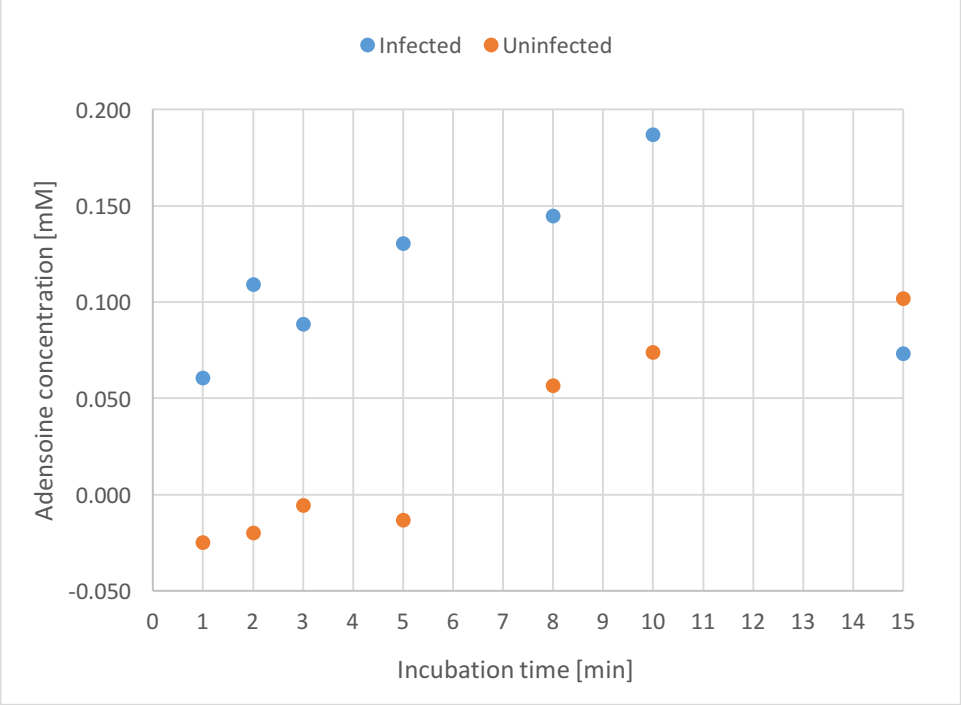


Figure 14: Comparison of adenosine concentrations after certain incubation times between infected and uninfected larvae for 0.15mM EHNA

Table 14: Measured values of the adenosine concentration in dependence of time for 0.1mM EHNA

| Infection | Incubation time [min] | Absorption (A570nm); Measurement: | | | | Absorption (A570nm) averaged | Adenosine Concentration [mM] |
|---|---|---|---|---|---|---|---|
| | | 1 | 2 | 3 | 4 | | |
| 0 | 1 | 0.091 | 0.259 | 0.23 | | 0.193 | 0.005 |
| 0 | 2 | 0.336 | 0.397 | 0.53 | | 0.421 | 0.027 |
| 0 | 3 | 0.405 | 0.524 | 0.402 | | 0.444 | 0.029 |
| 0 | 5 | 0.72 | 0.832 | 0.812 | | 0.788 | 0.062 |
| 0 | 8 | 0.323 | 0.241 | 0.623 | 0.594 | 0.445 | 0.029 |
| 0 | 10 | 0.678 | 0.794 | 0.78 | | 0.751 | 0.059 |
| 0 | 15 | 1.389 | 0.813 | 1.454 | | 1.219 | 0.104 |
| 1 | 1 | 0.03 | 0.106 | 0.122 | | 0.086 | -0.005 |
| 1 | 2 | 0.324 | 0.394 | 0.412 | | 0.377 | 0.023 |
| 1 | 3 | 0.6 | 0.769 | 0.787 | | 0.719 | 0.056 |
| 1 | 5 | 0.879 | 1.045 | 1.108 | | 1.011 | 0.084 |
| 1 | 8 | 0.545 | 0.698 | 0.724 | | 0.656 | 0.050 |
| 1 | 10 | 0.551 | 0.778 | 0.74 | | 0.690 | 0.053 |
| 1 | 15 | 0.489 | 0.672 | 0.551 | | 0.571 | 0.041 |

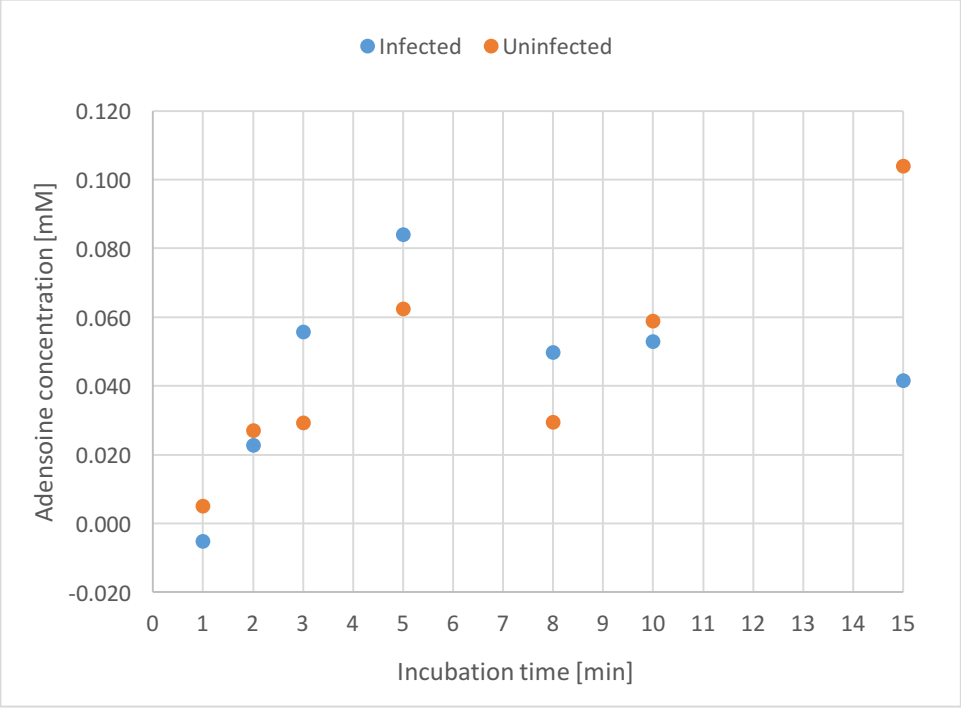


Figure 15: Comparison of adenosine concentrations after certain incubation times between infected and uninfected larvae for 0.1mM EHNA

Table 15: Measured values of the adenosine concentration in dependence of time for 0.05mM EHNA

| Infection | Incubation time [min] | Absorption (A570nm); Measurement: | | | Absorption (A570nm) averaged | Adenosine Concentration [mM] |
|---|---|---|---|---|---|---|
| | | 1 | 2 | 3 | | |
| 0 | 1 | -0.037 | 0.032 | 0.054 | 0.016 | 0.007 |
| 0 | 2 | 0.104 | 0.075 | 0.146 | 0.108 | 0.016 |
| 0 | 3 | 0.091 | 0.119 | 0.142 | 0.117 | 0.017 |
| 0 | 5 | 0.167 | 0.336 | 0.294 | 0.266 | 0.030 |
| 0 | 8 | 0.269 | 0.363 | 0.409 | 0.347 | 0.038 |
| 0 | 10 | 0.248 | 0.321 | 0.348 | 0.306 | 0.034 |
| 0 | 15 | 0.637 | 0.737 | 0.779 | 0.718 | 0.071 |
| 1 | 1 | -0.029 | 0.038 | 0.048 | 0.019 | 0.008 |
| 1 | 2 | 0.097 | 0.171 | 0.156 | 0.141 | 0.019 |
| 1 | 3 | 0.169 | 0.223 | 0.4 | 0.264 | 0.030 |
| 1 | 5 | 0.189 | 0.237 | 0.187 | 0.204 | 0.024 |
| 1 | 8 | 0.35 | 0.369 | 0.388 | 0.369 | 0.040 |
| 1 | 10 | 0.185 | 0.324 | 0.331 | 0.280 | 0.031 |
| 1 | 15 | 0.697 | 0.776 | 0.39 | 0.621 | 0.063 |

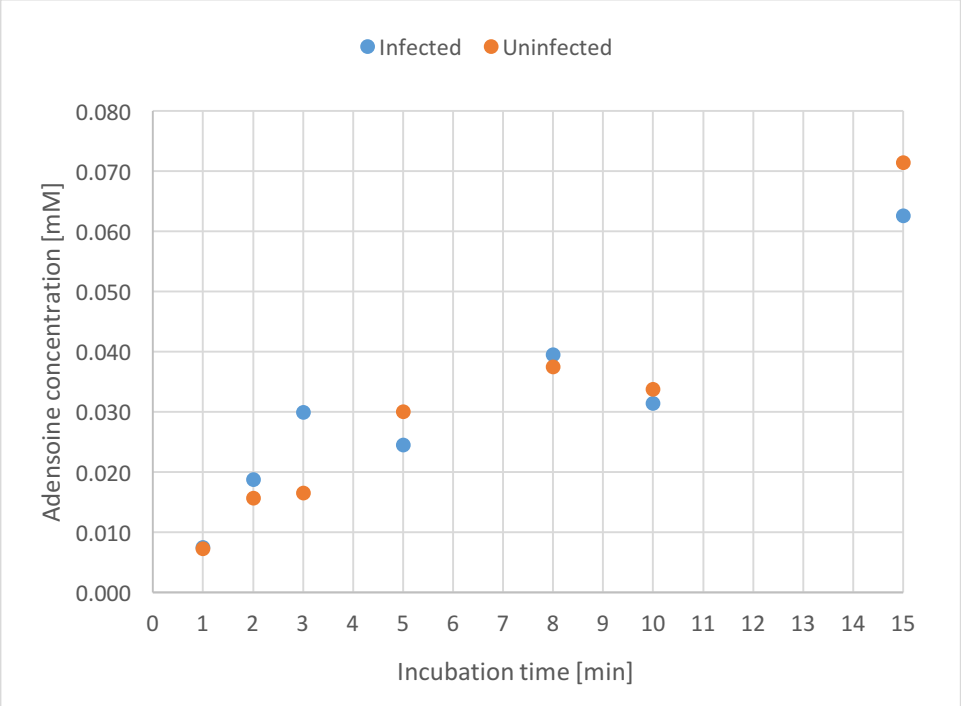


Figure 16: Comparison of adenosine concentrations after certain incubation times between infected and uninfected larvae for 0.05mM EHNA

Table 16: Measured values of the adenosine concentration in dependence of time for 0.025mM EHNA

| Infection | Incubation time [min] | Absorption (A570nm); Measurement: | | | Absorption (A570nm) averaged | Adenosine Concentration [mM] |
|---|---|---|---|---|---|---|
| | | 1 | 2 | 3 | | |
| 0 | 1 | 0.107 | 0.129 | 0.12 | 0.119 | 0.008 |
| 0 | 2 | 0.155 | 0.121 | 0.106 | 0.127 | 0.009 |
| 0 | 3 | 0.398 | 0.516 | 0.476 | 0.463 | 0.040 |
| 0 | 5 | 0.447 | 0.44 | 0.305 | 0.397 | 0.033 |
| 0 | 8 | 0.407 | 0.456 | 0.463 | 0.442 | 0.038 |
| 0 | 10 | 0.298 | 0.353 | 0.334 | 0.328 | 0.027 |
| 0 | 15 | 0.671 | 0.737 | 0.736 | 0.715 | 0.063 |
| 1 | 1 | 0.039 | 0.061 | 0.072 | 0.057 | 0.002 |
| 1 | 2 | 0.138 | 0.291 | 0.233 | 0.221 | 0.017 |
| 1 | 3 | 0.024 | 0.036 | 0.06 | 0.040 | 0.001 |
| 1 | 5 | 0.086 | 0.064 | 0.059 | 0.070 | 0.003 |
| 1 | 8 | 0.041 | 0.39 | 0.436 | 0.289 | 0.023 |
| 1 | 10 | 0.179 | 0.318 | 0.253 | 0.250 | 0.020 |
| 1 | 15 | 0.208 | 0.264 | 0.275 | 0.249 | 0.020 |

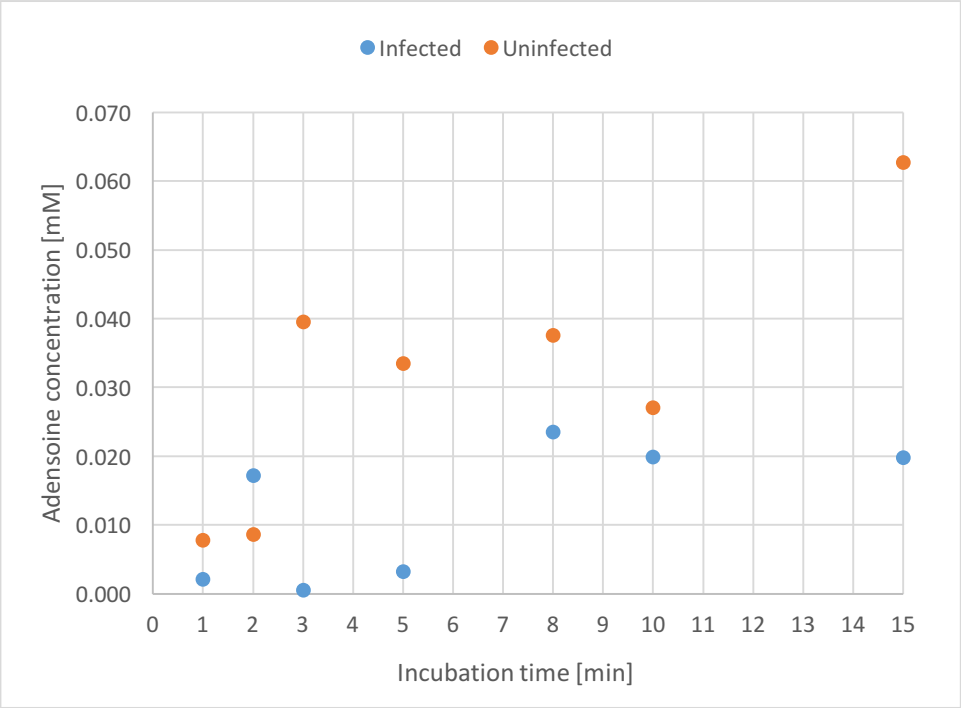


Figure 17: Comparison of adenosine concentrations after certain incubation times between infected and uninfected larvae for 0.025mM EHNA

Table 17: Measured values of the adenosine concentration in dependence of time for 0.015mM EHNA

| Infection | Incubation time [min] | Absorption (A570nm); Measurement: | | | Absorption (A570nm) averaged | Adenosine Concentration [mM] |
|---|---|---|---|---|---|---|
| | | 1 | 2 | 3 | | |
| 0 | 1 | 0.04 | 0.034 | 0.054 | 0.043 | 0.006 |
| 0 | 2 | 0.062 | 0.076 | 0.079 | 0.072 | 0.008 |
| 0 | 3 | 0.019 | 0.049 | 0.037 | 0.035 | 0.005 |
| 0 | 5 | 0.061 | 0.082 | 0.068 | 0.070 | 0.008 |
| 0 | 8 | 0.043 | 0.045 | 0.049 | 0.046 | 0.006 |
| 0 | 10 | 0.267 | 0.389 | 0.325 | 0.327 | 0.028 |
| 0 | 15 | 0.212 | 0.281 | 0.287 | 0.260 | 0.023 |
| 1 | 1 | 0.019 | 0.026 | 0.058 | 0.034 | 0.005 |
| 1 | 2 | 0.047 | 0.047 | 0.064 | 0.053 | 0.006 |
| 1 | 3 | 0.148 | 0.168 | 0.195 | 0.170 | 0.016 |
| 1 | 5 | 0.283 | 0.345 | 0.348 | 0.325 | 0.028 |
| 1 | 8 | 0.364 | 0.369 | 0.354 | 0.362 | 0.031 |
| 1 | 10 | -0.001 | 0.012 | 0.041 | 0.017 | 0.004 |
| 1 | 15 | 0.293 | 0.362 | 0.356 | 0.337 | 0.029 |

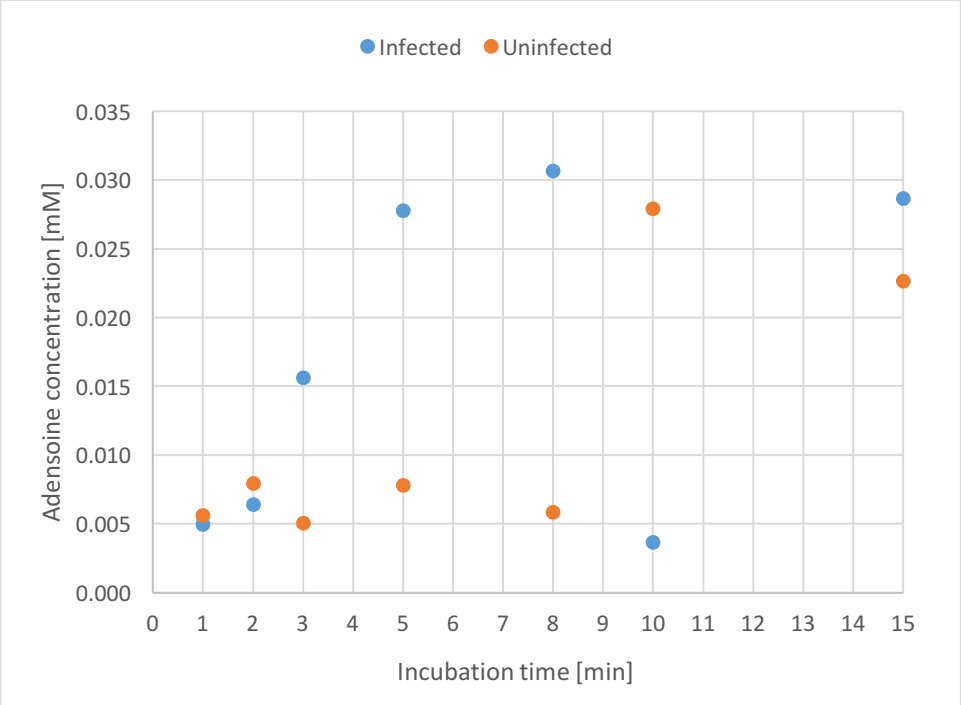


Figure 18: Comparison of adenosine concentrations after certain incubation times between infected and uninfected larvae for 0.015mM EHNA

# 10 Sample Preparation

## Preparation of Solutions

### PBS+6mM Trehalose+0.2mM Glucose:

**Glucose:**
c=0.2mM
V=10ml
M=198.17g/mol

First preparation of 1mg/ml solution (10mg in 10ml PBS) => concentration of 5.0462mM according to:

$$c = \frac{n}{V} = \frac{m}{M * V} = \frac{10 * 10^{-3} g}{198.17\,{}^{g}/_{mol} * 10 * 10^{-3} ml} = 5.0462 * 10^{-3} M = 5.0462 mM$$

Dilution to 0.2mM Glucose in PBS; V=10ml:

$$c_1 * V_1 = c_2 * V_2$$

$$V_2 = \frac{c_1 * V_1}{c_2} = \frac{0.2mM * 10ml}{5.0462mM} = 0.396ml = 396\mu l$$

$396\mu l$ of the 1mg/ml solution diluted with 9.604ml of pure PBS.

**Trehalose:**
c=6mM
V=10ml
M=378.33g/mol

$$m = M * c * V = 378.33\,{}^{g}/_{mol} * 6 * 10^{-3} M * 10 * 10^{-3} l = 0.02269 g$$

Dissolve 0.02269g Trehalose in PBS with already 0.2mM Glucose.

Adaption for 50ml: 1.980ml of 1mg/ml Glucose Solution
0.11345g Trehalose
48.02ml PBS

### PBS+6mM Trehalose+0.2mM Glucose+1mM Adenosine:

Prepare PBS+6mM Trehalose+0.2mM Glucose as described above (10ml).

**Adenosine:**
c=1mM
V=10ml
M=267.25g/mol

$$m = M * c * V = 267.25\,{}^{g}/_{mol} * 1 * 10^{-3} M * 10 * 10^{-3} l = 0.0026725 g$$

Dissolve 0.0026725g Adenosine in 10ml of PBS+6mM Trehalose+0.2mM Glucose.

## PBS+6mM Trehalose+0.2mM Glucose+1mM Inosine:

Prepare PBS+6mM Trehalose+0.2mM Glucose as described above (10ml).

### Inosine:

c=1mM
V=10ml
M=268.23g/mol

$$m = M * c * V = 268.23\,{}^{g}/_{mol} * 1 * 10^{-3}M * 10 * 10^{-3}l = 0.0026823g$$

Dissolve 0.0026725g Inosine in 10ml of PBS+6mM Trehalose+0.2mM Glucose.

## PBS+6mM Trehalose+0.2mM Glucose+0.5mM Adenosine:

Prepare PBS+6mM Trehalose+0.2mM Glucose as described above (10ml).

### Adenosine:

c=0.5mM
V=10ml
M=267.25g/mol

$$m = M * c * V = 267.25\,{}^{g}/_{mol} * 0.5 * 10^{-3}M * 10 * 10^{-3}l = 0.001336g$$

Dissolve 0.001336g Adenosine in 10ml of PBS+6mM Trehalose+0.2mM Glucose.

## PBS+6mM Trehalose+0.2mM Glucose+0.15mM EHNA:

Prepare PBS+6mM Trehalose+0.2mM Glucose as described above (25ml).

### EHNA:

c=0.15mM
V=25ml
M=313.83g/mol

$$m = M * c * V = 313.83\,{}^{g}/_{mol} * 0.15 * 10^{-3}M * 25 * 10^{-3}l = 0.00118g$$

Dissolve 0.00118g EHNA in 10ml of PBS+6mM Trehalose+0.2mM Glucose.

## PBS+6mM Trehalose+0.2mM Glucose+0.1/0.05/0.025/0.015mM EHNA:

Prepare PBS+6mM Trehalose+0.2mM Glucose as described above (at least 20ml).
Prepare PBS+6mM Trehalose+0.2mM Glucose+0.15mM EHNA as described above (at least about 7ml).

### EHNA:

c=0.1mM
V=5ml

$$c_1 * V_1 = c_2 * V_2$$

$$V_2 = \frac{c_1 * V_1}{c_2} = \frac{0.1mM * 5ml}{0.15mM} = 3.333ml$$

Dilute 3.333ml PBS+6mM Trehalose+0.2mM Glucose+0.15mM EHNA with 1.666ml PBS+6mM Trehalose+0.2mM Glucose.

c=0.05mM
V=5ml

$$c_1 * V_1 = c_2 * V_2$$

$$V_2 = \frac{c_1 * V_1}{c_2} = \frac{0.05mM * 5ml}{0.15mM} = 1.666ml$$

Dilute 1.666ml PBS+6mM Trehalose+0.2mM Glucose+0.15mM EHNA with 3.333ml PBS+6mM Trehalose+0.2mM Glucose.

c=0.025mM
V=5ml

$$c_1 * V_1 = c_2 * V_2$$

$$V_2 = \frac{c_1 * V_1}{c_2} = \frac{0.025mM * 5ml}{0.15mM} = 0.833ml$$

Dilute 0.833ml PBS+6mM Trehalose+0.2mM Glucose+0.15mM EHNA with 4.166ml PBS+6mM Trehalose+0.2mM Glucose.

c=0.015mM
V=10ml

$$c_1 * V_1 = c_2 * V_2$$

$$V_2 = \frac{c_1 * V_1}{c_2} = \frac{0.015mM * 10ml}{0.15mM} = 1ml$$

Dilute 1ml PBS+6mM Trehalose+0.2mM Glucose+0.15mM EHNA with 9ml PBS+6mM Trehalose+0.2mM Glucose.

# Adenosine Calibration Curves

## Preparation PBS+0.2mM Glucose+6mM Trehalose+0.15/0.1/0.05/0.025/0.015mM EHNA+0.5mM Adenosine (Standards):

Prepare PBS+6mM Trehalose+0.2mM Glucose+0.15mM EHNA as described above (10ml).
Prepare PBS+6mM Trehalose+0.2mM Glucose+0.5mM Adenosine (about 5ml should be way enough).

### 0.15mM EHNA+0.5mM Adenosine:

c=0.5mM
V=5ml
M=267.25g/mol

$$m = M * c * V = 267.25\,{}^{g}/_{mol} * 0.5 * 10^{-3}M * 5 * 10^{-3}l = 0.000668g$$

Dissolve 0.000668g Adenosine in 10ml of PBS+6mM Trehalose+0.2mM Glucose+0.15mM EHNA.

### 0.5mM Adenosin+0.1/0.05/0.025/0.015mM EHNA:

c=0.1mM
V=1ml

$$c_1 * V_1 = c_2 * V_2$$

$$V_2 = \frac{c_1 * V_1}{c_2} = \frac{0.1mM * 1ml}{0.15mM} = 0.666ml$$

Dilute 0.666ml PBS+6mM Trehalose+0.2mM Glucose+0.15mM EHNA+0.5mM Adenosine with 0.333ml PBS+6mM Trehalose+0.2mM Glucose+0.5mM Adenosine.

c=0.05mM
V=1ml

$$c_1 * V_1 = c_2 * V_2$$

$$V_2 = \frac{c_1 * V_1}{c_2} = \frac{0.05mM * 1ml}{0.15mM} = 0.333ml$$

Dilute 0.333ml PBS+6mM Trehalose+0.2mM Glucose+0.15mM EHNA+0.5mM Adenosine with 0.666ml PBS+6mM Trehalose+0.2mM Glucose+0.5mM Adenosine.

c=0.025mM
V=1ml

$$c_1 * V_1 = c_2 * V_2$$

$$V_2 = \frac{c_1 * V_1}{c_2} = \frac{0.025mM * 1ml}{0.15mM} = 0.166ml$$

Dilute 0.166ml PBS+6mM Trehalose+0.2mM Glucose+0.15mM EHNA+0.5mM Adenosine with 0.833ml PBS+6mM Trehalose+0.2mM Glucose+0.5mM Adenosine.

c=0.015mM
V=1ml

$$c_1 * V_1 = c_2 * V_2$$

$$V_2 = \frac{c_1 * V_1}{c_2} = \frac{0.015mM * 1ml}{0.15mM} = 0.1ml$$

Dilute 0.1ml PBS+6mM Trehalose+0.2mM Glucose+0.15mM EHNA+0.5mM Adenosine with 0.9ml PBS+6mM Trehalose+0.2mM Glucose+0.5mM Adenosine.

## Dilution steps for the calibration points:

Prepare the standards as described above (1ml).
Prepare PBS+6mM Trehalose+0.2mM Glucose+0.15/0.1/0.05/0.025/0.015mM EHNA for dilution (each about 1ml maximum).

Dilutions for 0.35/0.25/0.1/0.08/0.05/0.035/0.025/0.01mM Adenosine from 0.5mM Adenosine solutions.

| Adenosine concentration | Dilution PBS+sugars+EHNA+Adenosine:PBS+sugars+EHNA |
|---|---|
| 0.35mM | 7:3 |
| 0.25mM | 1:1 |
| 0.1mM | 1:4 |
| 0.08mM | 16:84 |
| 0.05mM | 1:9 |
| 0.035mM | 7:93 |
| 0.025mM | 5:95 |
| 0.01mM | 2:98 |

Principle:
c=0.035mM (desired)
c=0.5mM (available)
V=100ml

$$c_1 * V_1 = c_2 * V_2$$

$$V_2 = \frac{c_1 * V_1}{c_2} = \frac{0.035mM * 100ml}{0.5mM} = 7ml$$

Dilute 7ml PBS+6mM Trehalose+0.2mM Glucose+ EHNA+0.5mM Adenosine with 93ml PBS+6mM Trehalose+0.2mM Glucose+ EHNA.
Dilute in ratio 7:93.